Astronomical and Astrophysical Transactions (*AApTr*), 2024, Vol. 34, Issue 4, pp. 299–316,
ISSN 1055-6796, Photocopying permitted by license only, ©Cambridge Scientific Publishers

Space weather effects in Odesa magnetic anomaly – analysis by neural networks and wavelet methods

M.I. Ryabov[1,*], A.L. Sukharev[1], M.I. Orlyuk[2], D.M. Ryabov[3], Yu.P. Sumaruk[2], A.O. Romenets[1,2], E.M. Strakhov[4], D. Zabora[1]

[1] *Odesa Observatory "URAN-4", Radio Astronomy Institute of the National Academy of Sciences of Ukraine, Odesa, Ukraine*
[2] *S.I. Subbotin Institute of Geophysics of the National Academy of Sciences of Ukraine, Odesa, Ukraine*
[3] *Scientific-research Institute of Info Communication of A.S. Popov Odessa National Academy of Telecommunications, Odesa, Ukraine*
[4] *Odesa I.I. Mechnikov National University, Faculty of Mathematics, Physics and Information Technologies, Odesa, Ukraine*

Received 12 March, 2024; accepted 12 May, 2024

Analysis of large time series of geomagnetic data obtained at the Odessa and Lviv geomagnetic observatories in Ukraine reveals the difficulty of determining geomagnetic (including sudden) storms. Calculation of traditionally used K-indexes has some disadvantages: they provide no link to the physical features of magnetic storms' development, do not account for their duration, and evaluate geomagnetic activity only in three-hour intervals. Here we considered the use of neural network clustering and wavelet analysis for detecting geomagnetic storms in large data series over one or several months. We used a self-learning neural network (Kohonen Map), attracting data of the INTERMAGNET catalog (Lviv magnetic station) for June and July 2023. Automatic neural network clustering was found to effectively single out from a large array of data exactly the events with bursts of geomagnetic variations (on components X, Y, Z of geomagnetic field), which most often correspond to phases of magnetic storms' development. Additionally, the wavelet method for constructing global wavelet power spectra with frequency averaging (spectral power distribution over time) was considered. High-amplitude bursts in global wavelet spectra also usually correspond to bursts in geomagnetic variations during storms. This is a relatively simple and good visual method for quickly assessing the occurrence and duration of magnetic storms. Disadvantages leading to incorrect determination of the occurrence of some magnetic storms were also considered. The described methodology has become useful for the work on compiling a "catalog of geomagnetic storms", which is carried out using magnetometric monitoring data in the area of the Odessa regional magnetic anomaly (Ukraine).

Keywords: Geomagnetic field, space weather, geomagnetic storms, geomagnetic anomaly, neural network

*Email: ryabov-uran@ukr.net

1 Introduction

On the territory of Ukraine there are three geomagnetic observatories at the S.I. Subbotin Institute of Geophysics, NAS of Ukraine – "Lviv", "Kyiv" and "Odesa" [1]. These observatories have a large number of observations datasets of the Earth's magnetic field, which makes it possible to characterize magnetic activity during different periods of Solar activity. Of particular interest is the availability of unique long-term monitoring data on the dynamics of geomagnetic storms in the region of the large Odessa Regional Magnetic Anomaly (ORMA). The study of the properties and features of the dynamics of geomagnetic disturbances in the area of this magnetic anomaly is carried out jointly by the S.I. Subbotin Institute of Geophysics (IGP) and the Radio Astronomy Institute, National Academy of Sciences of Ukraine (IRA NASU). As a result, a catalog of geomagnetic storms in the ORMA region was created and is constantly being updated [2]. Based on the results of an analysis of the features of the manifestation geomagnetic storms in the ORMA region and planetary storms in the 22 and 23 cycles of Solar activity, it was shown that the magnetic anomaly enhances the regional manifestations of planetary magnetic storms [3]. A comparative analysis showed that the duration of magnetic storms in the ORMA region is on average longer than the duration of planetary storms. In this regard, studying the influence of this anomaly on the dynamics of the development of geomagnetic storms and ionospheric disturbances is an important and actual scientific task.

Because the work uses large amounts of data (more than a month in duration, with every second/every minute measurements), the identification of geomagnetic storms and disturbances (especially with appearance of rapid geomagnetic variations) becomes difficult. The calculation of the K-index, traditionally used for this purpose, is inconvenient for this work, since the K-index has no physical connection with the properties of a magnetic storm and is calculated for three-hour time intervals. Since both magnetic storms and small disturbances are often (but not always) accompanied by quasi-periodic variations in the geomagnetic field, it is necessary to apply modern data processing methods that find and isolate such geomagnetic disturbances. This is important for further study of the properties and features of geomagnetic variations as a response to the magnetic storms of different nature and intensity. Presently, many different methods for determining K indices have been developed. The most common of them, which is used when processing geomagnetic records of observatories of the global INTERMAGNET network, is described in [4]. One of the interesting modern methods of analysis, tested in this work, is the use of a neural network for automatic clustering of input data variations Bx, By, Bz – components of the geomagnetic field, in the "unsupervised learning" option, taking into account the features of the data structure.

2 Materials and methods

2.1 Odessa regional geomagnetic anomaly

ORMA was discovered and first described based on the results of magnetometric measurements around Odesa at the end of the 19th century [5]. The visualization of ORMA was presented in [6], and its modern image can be seen on the relief map of the induction module of the geomagnetic field B for the territory of Ukraine (Figure 1).

Currently, this anomaly is described in a number of publications, for example [7, 8]. In accordance with them, it has a complex structure and is characterized by intense positive anomalies (up to a few thousand nanotesla). The North of the territory is characterized by isometric or slightly elongated (in the NorthWest direction) anomalies with an intensity of 1000–10,000 nT. In the South of the territory, ORMA is confined to the Odessa Fault zone. In general, the ORMA in the maximum zone has an intensity of about 700 nT [9]. This anomaly has a deep nature and is associated with sources with a magnetization of 2.0–4.0 A/m, lying deeper than 10 km [10]. The anomaly source model consists of blocks with vertical and inclined side faces located at depths from 1 to 7 km (sources of local magnetic anomalies) and 7–40 km (sources of regional anomalies). The magnetization of the blocks varies from 0.7 A/m for the background body to 3.5–4 A/m directly for the sources of the anomaly. The ORMA's area is limited and controlled by deep faults of different ages and the boundaries of superimposed structures and is located in the currently geologically active zone of the North–NorthWest-trending Odessa fault. Therefore, it can manifest itself in the dynamics of the geomagnetic field in general and its variations in particular. In general, for Ukraine, and for the ORMA territory in particular, there has been a significant

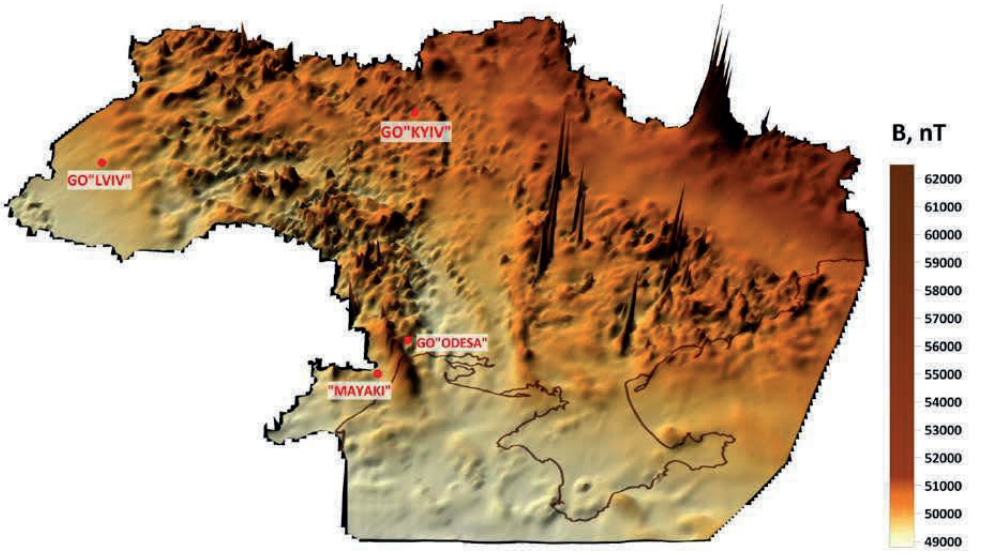


Figure 1 3D visualization of the geomagnetic field induction B on the territory of Ukraine (for 2005) and the location of three geomagnetic observatories "Lviv", "Kyiv" and "Odesa" and the new geomagnetic monitoring station located in the Mayaki village (Odessa region).

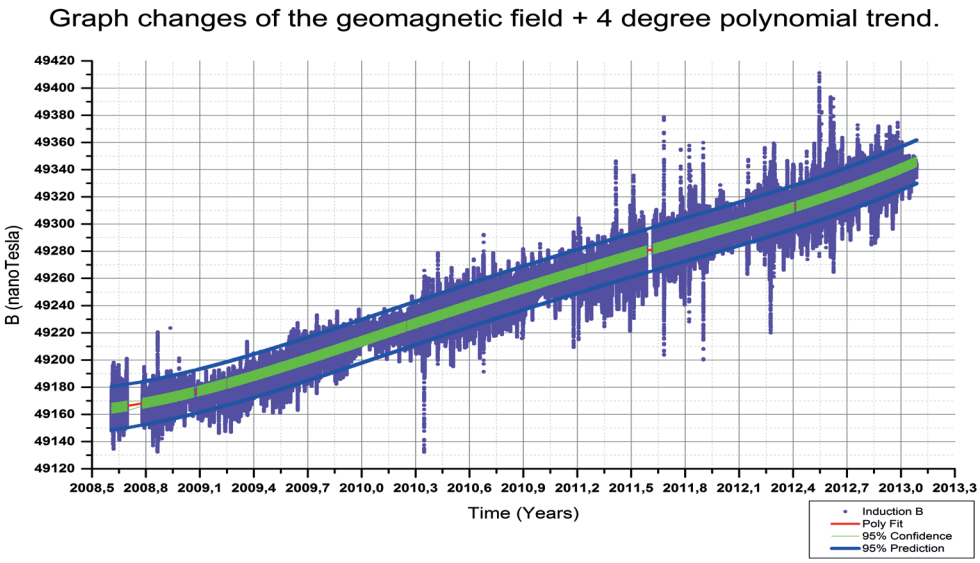


Figure 2 The type of the change in the modulus of induction of the geomagnetic field B at the Odessa geomagnetic observatory (the Stepanovka village in the Odessa region). The graph shows a 4th degree polynomial trend with 95% confidence and prediction intervals. The figure shows that from 2008 to 2013, geomagnetic induction increased by approximately 180 nT.

increase in the geomagnetic field induction module from 1950 to the present time [11]. An example of the trending multi-year increase of geomagnetic field induction in ORMA, from 2008 to 2013, is shown in Figure 2.

Currently, measurements of the variational components of the geomagnetic field have been carried out at different points in the ORMA region: at the Odessa geomagnetic observatory (located in the Stepanovka village), directly in the Odessa city, as well as in the Mayaki village (about 38 km SouthWest from the Odessa city), next to the low-frequency phased array (radio telescope) "URAN-4".

2.2 Clustering of geomagnetic monitoring data using a Kohonen neural network

To test the use of automatic detection of geomagnetic disturbances with short-periodic variations, a clustering method based on a neural network of the "Kohonen map" type was tested. It was applied to large observational dataset of the geomagnetic field with a sampling rate of 1 minute both in the ORMA region and in the Lviv RMA region (Geomagnetic Observatory "Lviv"). The fact is that in the problem we are solving there is no explicit indication of the standard rules for classifying the analyzed data. It is known that the Kohonen neural network is capable of independently organizing its structure and adapting to changes in input data. This neural network can discover hidden patterns and structure in data without the need to explicitly specify rules (unsupervised learning). The main idea of this neural network was proposed by the Finnish scientist Teuvo Kohonen. Currently, a competitive neural network with

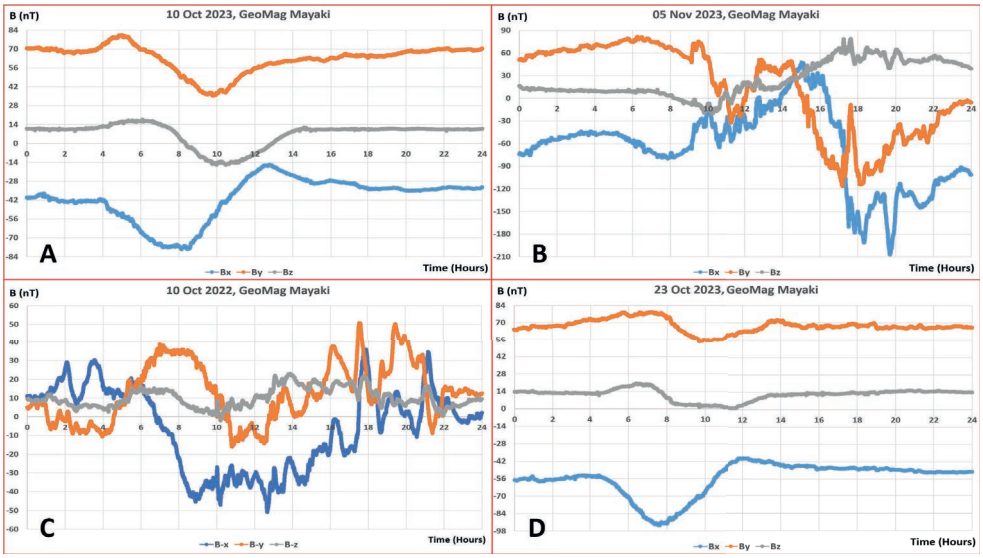


Figure 3 Examples of records of a quiet (Figures A (10/10/2023), D (10/23/2023)) and disturbed (Figures C (10/10/2022), B (11/05/2023)) geomagnetic field (Mayaki village).

unsupervised learning (self-organizing feature map (SOFM)) is popular in problems of visualization and clustering of various experimental data, but has not yet been applied in Ukraine to geomagnetism data in the format of our task.

Figure 3 shows examples of a calm and disturbed geomagnetic field in the ORMA region (Mayaki village). As can be seen in the figure, many geomagnetic disturbances are accompanied by the appearance of short-periodic "bursts" in variations of the *Bx*, *By*, *Bz* components of the geomagnetic field.

In this example, it is clearly seen that during geomagnetic disturbances short-periodic variations of the geomagnetic field appear on three *X*, *Y*, *Z* coordinates (most often in the time interval from 1.5–2–4 hours to 30 minutes), which can be used as markers for automatic recognition of them, and therefore, determination of days in which there were geomagnetic disturbances.

Therefore, an amplification in such short-period variations may be a sign of geomagnetic disturbance, although not in all cases. In this case, clustering using SOFM can highlight areas of time series *Bx*, *By*, *Bz* components of geomagnetic field variations where there were bursts of short-periodic variations. Because the methodology, as well as similar examples of implementation and application of the Kohonen map neural network, are discussed in detail in many works [12–14], therefore, we show only the basic principle of operation of neural networks of this type.

The work of the Kohonen neural network begins with initialization, that is, the initial assignment of neuron weight vectors. This is followed by a cycle: 1) selecting the next observation in the form of a vector from the input data; 2) finding the best matching neuron (BMU – Best Matching Unit) for it, that is, the neuron on the map whose weight vector is least different from the observation (usually in the Euclidean metric); 3) determining the number of BMU neighbor neurons and training, that is,

changing the weight vectors of the BMU and neighbors to better approximate them to the observation; 4) determining the map calculation error. Accordingly, the basic calculation algorithm is: initializing the initial weights of neurons by setting all coordinates to random numbers or (preferably) assigning a weight vector to a random value from the input data; cyclic iterations: t – iteration number (initialization corresponds to zero number). Next, we need to select a random observation *x(t)* from the input data, find the distances from it to the weight vectors of all neurons in the map and determine the neuron closest in weight $M_c(t)$, this will be BMU. There is a condition for it $\|x(t) - m_c(t)\| \leq \|x(t) - m_i(t)\|$ for any $m_i(t)$ – neuron weight vector $M_i(t)$. If there are several neurons that satisfy this condition, then the BMU is randomly selected among them. Next, we need to determine using the neighborhood function h, neighbors of a neuron M_c and the magnitude of changes in their weight vectors. The function h determines the measure of the neighborhood of neurons M_i and M_c as well as changing weight vectors. This function should gradually refine their values, first stronger for a larger number of neurons, then weaker for a smaller number of neurons. Typically, a Gaussian function is used for the neighborhood function of the form $h_{c\ i}(t) = \alpha(t)e^{\left(-\frac{\|r_c - r_i\|^2}{2\sigma^2(t)}\right)}$, where $0 < \alpha(t) < 1$ – training factor that monotonically decreases with each subsequent iteration, in other words, it determines the approximation of the value of the weight vectors of the BMU and its neighboring neurons to the observation, and the larger the step, the smaller the refinement; r_i , r_c – neuron coordinates $M_i(t)$, $M_c(t)$ on the map; $\sigma(t)$ – the factor that reduces the number of neighboring neurons with iterations decreases monotonically. Parameters α, σ and their type of decrease is set by the researcher. Sometimes a simplified form of the neighborhood function is used in the form $h_{c\ i}(t) = \alpha(t)$ if $M_i(t)$ located in the vicinity $M_c(t)$ with a given radius, and 0 in the negative case. Function $h(t)$ equal to $\alpha(t)$ for BMU and decreases with distance from BMU. Next comes a change in the neuron weight vectors: $m_i(t) = m_i(t-1) + h_{c\ i}(t)(x(t) - m_i(t-1))$ and thus, the weight vectors of all neurons that are adjacent to the BMU approach the observation in question. Finally, the map computation error is calculated, most often in the form of the average of the distances between observations and the weight vectors corresponding to their BMU: $\frac{1}{N}\sum_{i=1}^{N}\|x_i - m_c\|$ where N is the number of elements of the input data [15].

2.3 Continuous wavelet analysis in search for geomagnetic disturbances in monitoring data

For an alternative method of searching for geomagnetic storms and disturbances, the method of constructing a global wavelet spectrum was used by averaging a matrix of continuous wavelet transform coefficients over frequency. The "fast" wavelet transform method was used, which uses FFT (Fast Fourier Transform), because the continuous wavelet transform can be represented as a convolution of a sequence of input data with a set of functions generated by the analyzing wavelet. Convolution can be calculated using FFT [16]. To calculate the wavelet transform, a Morlet wavelet with wave number 12 (the number of "waves" of the wavelet function) with an FFT length of 131072 frequencies was used. Next, a spectral power curve was

calculated, representing snapshots of signal strength between specified frequencies in time (300 time steps were used to construct the global spectrum curve). The global spectrum with frequency averaging shows the distribution of the spectral power of the signal over time, and is convenient for determining the moments of greatest activity of the signal under study, that is, the moments of the best comparison of the analyzing wavelet and the signal at different frequencies/periods in the same time interval. Bursts of spectral power thus most often correspond to moments in time of geomagnetic disturbances, although this is not always the case.

It should be noted that before the start of wavelet analysis, the data of X, Y, Z coordinates of the geomagnetic field were filtered in a period band of 12 hours – 5 minutes using a band-pass FFT filter [17]. This allows us to analyze only the contribution of fast short-periodic variations to the overall variability of geomagnetic data and remove the slow trend in the data and interfering fluctuations with periods of several days.

3 Results

3.1 Neuroclusterization

Next, we consider some results of training and testing of the Kohonen neural network in relation to monitoring data on changes in the geomagnetic field, which were obtained at the Ukrainian geomagnetic observatories "Lviv" and "Odessa" (with a time resolution of 1 min). Data from the Lviv observatory were obtained from the international open network of geomagnetic observatories INTERMAGNET. Geomagnetic measurements were obtained using precision fluxgate magnetometers (three-component) LEMI-008 produced by LC ISR (Lviv Center of the Space Research Institute), FGM (Flux Gate Magnetometer) produced by DMI (Danish Metrological Institute) and TPM produced by the Institute of Geophysics PAS (Polish Academy of Sciences).

For automatic clustering, a Kohonen neural network with a map consisting of 64 neurons (8x8) was used, while the original data was randomly divided into three samples: train (which contained 70% of the data) and test (15% of the data), validation (15% of data). This is necessary to improve the quality of the neural network, that is, the ability to predict (distribute) data that was not used during training. A common problem is "overtraining" of a neural network, when the training data has been reproduced so completely that even noise within individual data sets is reproduced, which sharply reduces the ability of the neural network to make correct predictions (distributions) of new data sets. To avoid this problem, a good way is to divide the source data into three parts: training set, test set, validation set. These samples can be used to fundamentally train the neural network, validate (testing) the success of the neural network during training, and perform a final validation test to determine how well the network predicts "new" data that was not used to train the model or test its success during training. The number of iterations when calculating clustering was 7000 steps, the initial neighborhood of the winning neuron was 3 cells. Let us consider the results obtained. It is worth noting that before starting the analysis, the following preparatory steps were carried out: subtraction of the average values of the

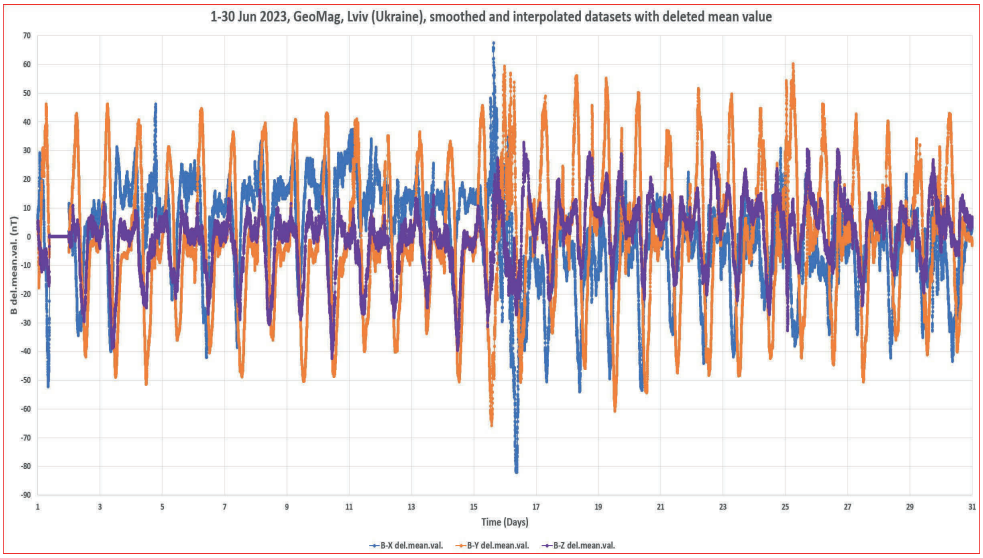


Figure 4 Record of *Bx*, *By*, *Bz* – variations of geomagnetic induction (after interpolation, smoothing and subtraction of average induction values) for January 1–30, 2023, which was obtained at the "Lviv" geomagnetic observatory.

X, *Y*, *Z* components of the geomagnetic field, followed by interpolation and smoothing using a cubic spline (smoothing is determined using the cross-validation procedure) [18]. This allows avoiding distortions in training and subsequent application of the neural network, caused by random noise in the data. The initial training of the neural network took place using data from June 2023 (Lviv Observatory). Next, the already trained neural network analyzed data for February–March 2023 and a short fragment of data for July 1–14, 2023, with noise (to understand the neural network's resistance to noise). An example dataset for June 2023 is shown in Figure 4.

The results of cluster analysis were obtained, where, after training on the structure properties of the analyzed geomagnetic field data, neurons distributions of data elements were obtained into separate 64 clusters in an 8×8 grid (Kohonen maps). Examples of Kohonen maps of the obtained clusters and distribution the number of data points included in the clusters, for time series 1–14 July and 1–30 June 2023, are shown in Figure 5. Moreover, if we combine the data from all 64 clusters, we will get a model series that is very close to the input data. Of interest in such maps are the clusters in which the largest amount of data is collected. Often this means that the neural network has found some interconnected structure in the input data, in this case, which manifests itself in the *X*, *Y*, *Z* series of geomagnetic field variations. In this sense, the neural network resembles an adaptive filter that allows us to find and highlight orderly elements of geomagnetic data.

In order to see which data were distributed into clusters as a result of the analysis, it is necessary to visualize the "contents" of the neurons that received the largest number of cases. An example is shown in Figure 6. For data July 1–14, 2023, the contents of the main cluster are visualized, and for data June 1–30, 2023, the contents

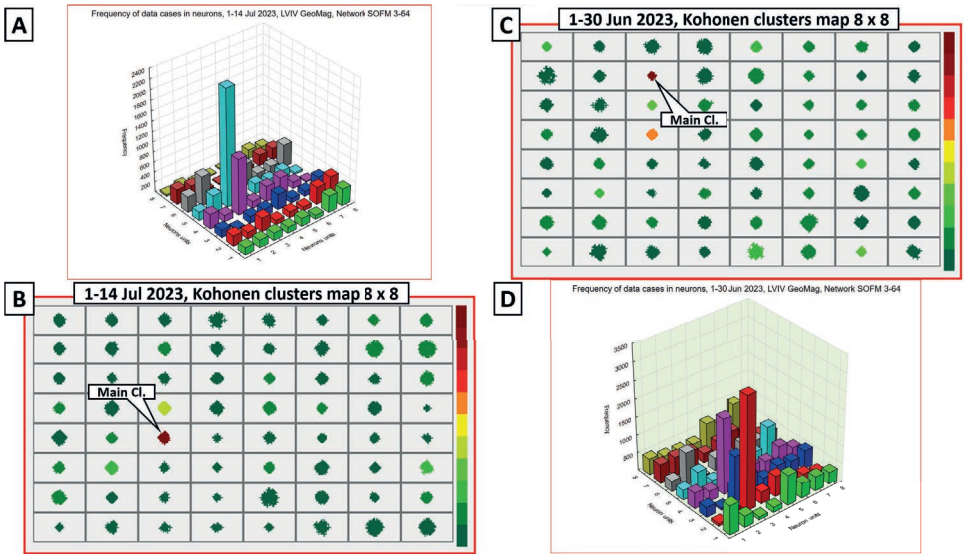


Figure 5 The result of cluster analysis using the example of data series 1–14 Jul and 30 Jun 2023: A) Histogram (for the data series 1–14 Jul 2023) of the hits number of elements of the analyzed data series into clusters. It can be seen that the neuron that occupies position (5, 3) on the 8 x 8 map has collected the largest number (2293) of elements. B) Map of the distribution of elements by clusters (Kohonen map) for the data series July 1–14, 2023. The winning neuron is marked by a flag. C) Kohonen map for data series June 1–30, 2023. The winning neuron is marked by a flag. D) Histogram (for the data series July 1–30, 2023) of the number of hits of elements of the analyzed data series into clusters; in this example, the largest number of elements (3162) corresponds to the neuron (2, 3). However, in addition to this neuron, the neuron at position (4, 3) collected 2092 data elements. Thus, *X*, *Y*, *Z* geomagnetic variations June 1–30, 2023 have a structure, mainly consisting from two groups of data.

of the main and second clusters are visualized. It is worth noting that in the data from July 1–14, 2023, a random distortion was left, which was on July 12, in order to test the neural network's response to the distortion. The example shows that indeed, the neural network primarily selects data blocks in which there were short-periodic variations in the geomagnetic field induction, or simultaneous bursts, at the *X*, *Y*, *Z* coordinates. The figures show areas that can be identified as geomagnetic disturbances. However, the neural network could not identify geomagnetic storms on July 8 and 14, 2023. At the same time, the strong interference, which appeared in the same time interval at *X*, *Y*, *Z* coordinates, was successfully identified. This fact is most likely due to the fact that on July 8 and 14 the geomagnetic storms did not contain simultaneous short-periodic variations in induction, and were distributed into clusters containing irregular variations in *Bx*, *By*, *Bz* data. A similar picture is observed when visualizing the contents of two clusters (the main and the second, according to an amount of selected elements) in the data of June 1–30, 2023. Small disturbances of the geomagnetic field, which were accompanied by pronounced rapid bursts, were clearly identified, but the magnetic storms of June 18 and 19 were unrecognized. Let

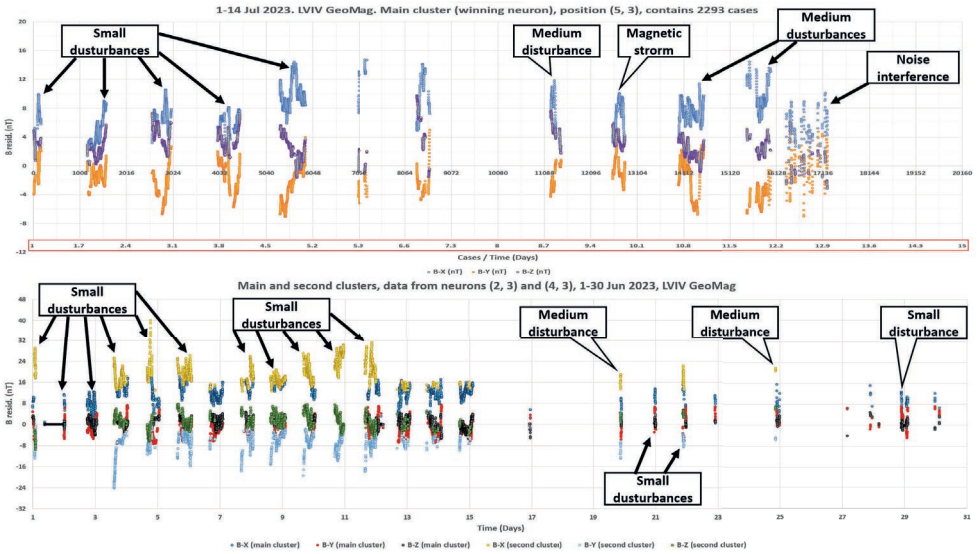


Figure 6 Example of data plots related to the main clusters obtained from the analysis. The top graph is July 1–14, 2023, the bottom graph is January 1–30, 2023. Fragments comparable to geomagnetic disturbances are shown by flags.

us look at this in more detail. Periodogram analysis (for uneven Lomb–Scargle series [19]) of main clusters showed that the time scale of variations is approximately 6–2 hours. Thus, the neural network identifies into main clusters mainly those fragments of geomagnetic disturbances in which variations increase with periods ranging from 6 to 2 hours. In the absence of these, individual bursts, fragments of an increase/decrease in signal amplitude are identified, or the method does not highlight anything in the case of time-shifted bursts on three coordinates. Although the Kohonen clustering method is considered to be quite resistant to interference, in practice, careful removal of noise and interference in the datasets is necessary to avoid creating a false effect of highlighting geomagnetic disturbances that would result from distortions.

Let us now consider neuroclustering for data obtained from the Odessa geomagnetic observatory in January 2019. This month there were no strong magnetic storms, but there were many small geomagnetic disturbances. Since the structure of geomagnetic induction variations in Stepanovka village is already different, a new neural network was trained on data for December 2018. The results are shown in Figure 7. As a result, SOFM identified the main cluster (8, 3) which included 7966 data elements. Visualization of the contents of this cluster showed the presence of many blocks, both short-periodic variations and individual bursts, mainly corresponding to a large number of weak geomagnetic disturbances, and some to weak magnetic storms. According to the results of the periodogram analysis, the time scale of variations, similar to the Lviv geomagnetic observatory, was approximately 6–5 – 3–2 hours. To take a closer look at the structure of geomagnetic induction variability in January 2019, wavelet spectrograms were constructed (data filtered by FFT, so that

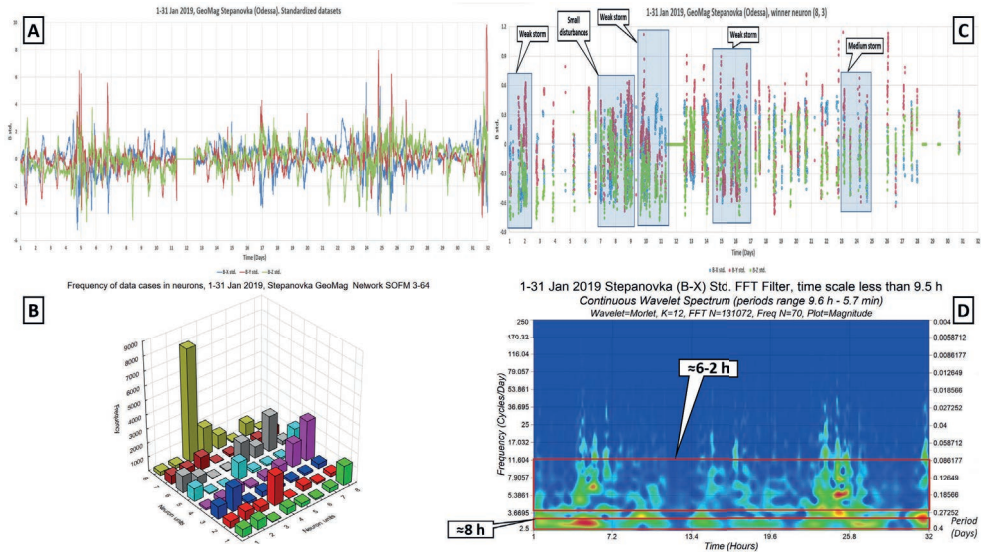


Figure 7 The example of neuroclustering observational data from the geomagnetic observatory "Odessa", January 2019. A) Initial smoothed and standardized X, Y, Z data. B) Histogram of the number of data cases selected by individual neurons. It can be seen that the neuron with position (8, 3) collected the largest amount of data (7966 elements). C) Visualization of data located in the main cluster. During January 2019, there were several small geomagnetic disturbances, which are highlighted in the figure, as well as weak geomagnetic disturbances, increased variations, mainly in the period range of 6–2 hours, which clustering was partially able to indicate. D) An example of a "continuous" wavelet spectrum (January 2019) for filtered data (Bx component of the geomagnetic field) in the band of 9.6 hours – 5.7 minutes, on which bands of periods about 8 hours (solar-diurnal variation) and 6–2 hours are marked by flags (which corresponds to the "periods" of variations detected by neuroclustering). It can be seen that the clustering method is more successful in those sections of the time series where variations close to quasiperiodic appear, and less successful where irregular, noise-like variations of the geomagnetic field appear.

the time scale of variations was less than 9.6 hours). It is clear from them that many weak geomagnetic disturbances have led to the fact that only the solar-daily period of about 8 hours is clearly visible, and the periods of 6 and 3 hours are significantly blurred, and in the band of periods 6–2 hours there is an overlap of regular and noise variations. As a result, SOFM identified some blocks corresponding to variations and bursts on three coordinates, while the magnetic storm on January 31, 2019 was not detected. As is known from previous studies of the dynamics of solar-diurnal variations in the ORMA region, the intensification of variations with periods in the range of 6–2 hours is noticeably greater during geomagnetic disturbances than in data from the Kiev geomagnetic observatory, and the amplitude bursts are 4–2 hours periods often correspond to weak geomagnetic disturbances better than according to the "Kiev" data [20]. This leads to the fact that SOFM preliminary identifies geomagnetic disturbances somewhat more clearly based on data obtained in the ORMA region, but this requires analysis of a larger amount of monthly data to clarify.

3.2 Global wavelet spectrum as an indicator of geomagnetic disturbances

As an additional method for searching manifestations of geomagnetic disturbances in data of geomagnetic field variations, we will consider the use of wavelet spectrograms and global spectra for this purpose. Wavelet spectrograms are an extremely convenient and effective for time-frequency visualization of geomagnetic variations and are widely used today in geophysics and space weather. Since the wavelet spectrum is a three-dimensional surface (time, frequency, magnitude), by averaging the matrix of wavelet transform coefficients along the time axis or frequency axis, one can obtain two types of so-called global wavelet spectra: the "frequency-spectral power" spectrum and the "time-spectral power" spectrum. The first is some analogue of a periodogram, the second shows the distribution of the spectral power of the signal over time. Many works are devoted to the practical application and features of global wavelet power spectra, for example [21, 22]. The frequency-averaged wavelet spectrum (based on the continuous wavelet transform) is a convenient method of analysis when it is necessary to find bursts in the spectral power of a signal caused by the "layering" of variability components over the same time interval, but with different time scales of variability, it is typical for multi-periodic signals, which are the data of geomagnetic field variations. Consider an example in Figure 8, built for May 2023 (data obtained at the Odessa Astronomical Observatory).

The maxima of the global wavelet spectrum correspond to an increase in the spectral power of the signal in a certain time interval, which is often caused by the appearance of multi-periodicity and the superposition of geomagnetic induction variations with different "periods" of variability. This also, in most cases, corresponds

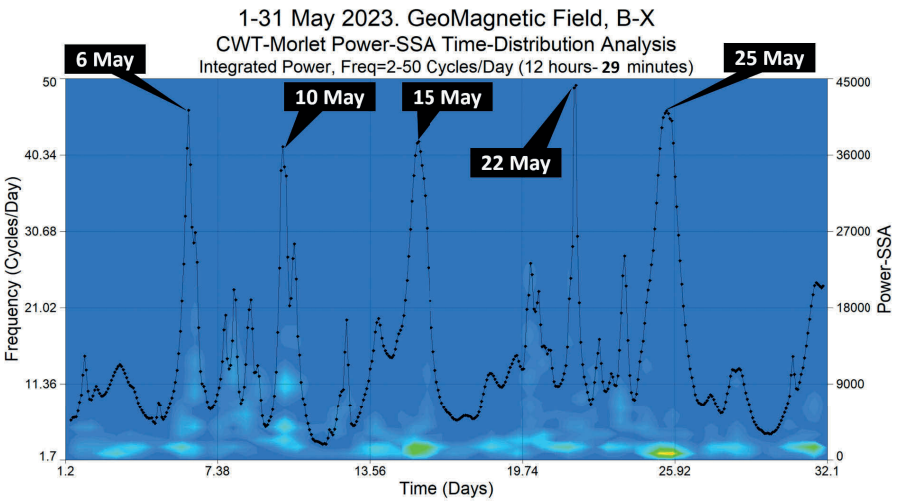


Figure 8 Global frequency-averaged wavelet spectrum (black graph) superimposed on a continuous wavelet spectrum constructed for variations in the *Bx* components of the geomagnetic field, May 1–31, 2023 (Odessa city). Flags indicate recognized geomagnetic storms and geomagnetic disturbances, corresponding to the maximums of the global wavelet power spectrum.

to the development of geomagnetic disturbances of varying intensity, especially in the ORMA region, where there is a slight predominance of short-periodic induction variations, on a time scale of less than 30 minutes, in comparison with other regions of Ukraine, where the geomagnetic field is close to normal. In this example, May 6, 10–11, 15 – magnetic storms, and May 22 and 25 – weak magnetic storms. Thus, the maxima of the power spectrum with frequency averaging of the wavelet transform matrix of the data coincide well with the dates of geomagnetic storms. In this case, time shifts of maxima can occur.

It is important that the global frequency-averaged wavelet spectrum allows us, in some cases, to recognize "noise" geomagnetic storms when broadband noise-like geomagnetic variations appear, since they also lead to an increase in spectral power in the time range of the storm. Using automatic detection of local maxima (as, for example, considered in [23]) it is possible to quickly determine the times of maxima of the global wavelet power spectrum, even in large data sets over several months, and thus determine the likely manifestation of geomagnetic disturbances of different intensities (and, accordingly, different spectral powers).

4 Discussion

Large regional magnetic anomalies in the Earth's lithosphere can appear (according to satellite data) at altitudes of about 100–300 km and even higher [24]. Thus, extensive magnetic anomalies can influence the formation and structure of plasma irregularities, forming a special response of the ionosphere to Solar activity events. Currently, this interrelation is very poorly studied, especially in Europe, mainly due to the lack of large low-frequency radio telescopes and permanent magnetometric stations in areas of magnetic anomalies. ORMA is distinguished by the fact that on its territory there is a low-frequency phased antenna array "URAN-4" (decameter radio range 10–30 MHz) for studying ionospheric scintillation of cosmic radio sources, as well as two magnetic observatories in different places of the magnetic anomaly (the Stepanovka village and the Mayaki village), which provides a unique opportunity to study the influence of a magnetic anomaly on the development of geomagnetic storms, short-periodic variations of the geomagnetic field and ionospheric scintillations of radio sources.

In this regard, the search and determination of geomagnetic disturbances, which are accompanied by an increase in short-periodic geomagnetic variations, is an important task, both for the work on filling the catalog of geomagnetic storms in Odessa, and for comparing data on geomagnetic and ionospheric activity in the ORMA region, taking into account the properties and features of the development of ionospheric scintillations in the decameter radio range. In addition, this is important for studying the similarities and differences in the development and evolution of short-periodic geomagnetic variations in the ORMA region and regions (Lviv, Kiev) where the geomagnetic field is close to normal, which appear during geomagnetic disturbances of various types caused by active processes on the Sun and propagation disturbances in geospace.

The study of the results of automatic cluster analysis (in relation to data from the Ukrainian geomagnetic observatories "Lviv" and "Odessa") using the Kohonen

neural network showed that, in relation to the analysis of three-coordinate X, Y, Z geomagnetic data obtained on three-component fluxgate magnetometers, the neural network recognizes features of structures geomagnetic variations. At the same time, the neural network works like a bandpass filter, distributing geomagnetic induction fluctuations into clusters on different time scales, from several hours to tens of minutes, and at different time intervals of manifestation in the source data. Analysis of data in the main clusters (those with the largest number of cases) showed that variations with "periods" of several hours predominate. In addition, the neural network identifies sharp spikes in the data, as well as areas of increase or decrease in geomagnetic induction occurring on three components. The latter are very uninformative. Geomagnetic disturbances, even quite strong ones, in which there are noise variations or no variations at all, are often not recognized by the Kohonen neural network.

A comparison of the results of clustering data obtained at the Lviv and Odessa observatories showed that geomagnetic disturbances are recognized more clearly using the Odessa observatory data. Most likely, this is caused by the fact that short-periodic quasi-harmonic variations in the range from several hours to tens of minutes, during geomagnetic disturbances in the ORMA region, occur more often [25, 26].

Considered in this work, an alternative additional method for searching and determining geomagnetic disturbances, based on the construction of global frequency-averaged wavelet power spectra based on the continuous wavelet transform, is a good method of visually determining geomagnetic disturbances. However, the "fast" method of calculating the matrix of wavelet coefficients using the Fourier transform used in the work requires a uniform time step in the source data, and preliminary filtering to remove the "slow" trend in the data and highlight geomagnetic variations on a 12-hour time scale – 5 minutes.

Summarizing the above, it should be noted that both methods – the Kohonen neural network and the global frequency-averaged wavelet power spectrum are better to determine those types of geomagnetic disturbances that contain short-periodic geomagnetic variations. This is an advantage, taking into account the tasks of the IGP and IRA NASU scientific group, in studying the properties of regional fast geomagnetic variations and their connection with ionospheric disturbances. The described methods have shown the possibility of their mutual complementation for exploration analysis in relation to geomagnetic data series ranging in length from a month to several months. However, in our case, the use of the traditional neuroclustering technique showed that noisy and "smooth" (without variations) geomagnetic disturbances are practically not recognized. Therefore, we will continue our experimental consideration of more advanced neuroclustering methods, in relation to datasets of geomagnetic variations.

Conclusions

- Application of the method of neuroclustering (by the Kohonen self-organizing feature map) of data variations of the geomagnetic field from observations at the geomagnetic observatories "Odessa" and "Lviv" has been studied to identify moments in time of the development of geomagnetic disturbances.

- It is shown that the contents of the main clusters correspond to individual bursts and intensification of geomagnetic field variations on a time scale of 6–2 hours. Since in the ORMA region, the increase in variations in the above period band coincides better with geomagnetic disturbances, neuroclustering of the "Odessa" data shows a slightly better identification of geomagnetic disturbances than in the case of data from the Lviv observatory.
- An alternative method for recognizing geomagnetic storms and disturbances is considered, based on the analysis of global wavelet spectra with frequency averaging (spectral power–time plot). This method is based on bursts of spectral power during time intervals when geomagnetic variations overlap with periods from several hours to tens of minutes or less, which often happens during geomagnetic storms. Unlike neuroclustering, this method can also recognize geomagnetic disturbances accompanied by broadband noise variations.
- The considered methods are based only on the analysis of the structure of time series *Bx*, *By*, *Bz* of records of geomagnetic field variations, without additional information, and will help in conducting exploratory analysis of archival data, for further study of the properties and features of the manifestation of geomagnetic disturbances and short-periodic variations in the ORMA region, in comparison with other regions of Ukraine.
- The combined use of the methods described in the article for determining the presence of geomagnetic disturbances in time series (X, Y, Z) of geomagnetic field variations allows us to identify the majority of such events and use them for more detailed consideration and analysis.

Author contributions

Yu.P. Sumaruk, provided data from geomagnetic observatories "Lviv" and "Odessa"; M.I. Ryabov, M.I. Orlyuk, A.O. Romenets, worked with the text of the article, necessary corrections and additions; D.M. Ryabov, E.M. Strakhov, helped with data processing using SOFM neuroclustering; A.L. Sukharev, main calculations and text of the article; D. Zabora, pre-processing of geomagnetic data and work with a catalog of geomagnetic storms.

Acknowledgments

The authors of the article express their gratitude to the team of the Institute of Geophysics NAS of Ukraine for their assistance in working on the article, the observation data provided, and valuable comments and additions. The authors are also grateful to the anonymous referees for their reviews, which helped to improve the article.

References

1. Yu.P. Sumaruk. Long-term changes in the geomagnetic field at magnetic observatories in Ukraine. Geophysical Journal, 2011, Vol. 33, No.5, P. 120–127 (in Russian)
2. L.I. Sobitnyak, M.I. Ryabov, M.I. Orlyuk, A.L. Sukharev, A.O. Romenets, Yu.P. Sumaruk, A.A. Pilipenko. Analysis of the Magnetic Storms Catalog for Monitoring Radio Source Flux Data with the URAN-4 Radio Telescope in the Odesa Magnetic Anomaly Zone. Radio Physics and Radio Astronomy, 2020, Vol. 25, No. 4, P. 324
3. L.I. Sobitnyak, M.I. Ryabov, M.I. Orlyuk, A.L. Sukharev, D.M. Ryabov, A. Romenets, Yu. Sumaruk. Comparative analysis of magnetic storms in the Odessa Magnetic Anomaly region with planetary and ionospheric storms during the monitoring program at RT "URAN-4" (1987-2010). Odessa Astronomical Publications, 2023, Vol. 36, P. 183
4. Nowozynski K., T. Ernst, J. Jankowski (1991). Adaptive smoothing method for computer derivation of K-indices. Geophys. J. Int., 1991, Vol. 104, No. 1, P: 85-93, DOI: 10.1111/j.1365-246X.1991.tb02495.x
5. S. Popruzhenko, "Odessa Magnetic Anomaly" ("Meteorological Review," ed. by Prof. A. V. Klossovsky, 1892, issue III) (in Russian)
6. Orlyuk M.I., Marchenko A.V., Romenets A.O., Bakarzhieva M.I. Development of digital maps of the induction module of the geomagnetic field $\boldsymbol{B}$ for the territory of Ukraine. 2023, Geophysics and geodynamics: forecasting and monitoring of the geological environment (Editor. V. Yu. Maksymchuk)., Lviv: Rastr-7., P. 152-155
7. Besutiu L., Pashkevich I., Orlyuk M., Besutiu G., Ivan M., Neaga V. Maglodan project. The first step in merging the national geomagnetic maps of Romania, Ukraine and Republic of Moldova. Tectonics and regional Geology, 1999, Vol. 77, Supplement No. 1, P. 66-67
8. Orlyuk M.I., Romenets A.A., Marchenko A.V., Orliuk I.M., Ivashchenko I.N. Magnetic declination on the territory of Ukraine: results of observations and calculations. Geoph. J., 2015, Vol.37, No. 2, P. 73-85, DOI: 10.24028/gzh.0203-3100.v37i2.2015.111307
9. Krutikhovskaya Z.A., Melnichuk E.V., Slonitskaya S.G., Orlyuk M.I. Regional magnetic anomalies and small-scale mineral forecasting. DAN USSR, 1985, No. 4, Ser. B., P. 37-43 (in Russian)
10. Pashkevich I.K., Karataev G.I., Orlyuk M.I. The structure of the lithosphere along geotraverse VIII. Magnetic field and magnetic model. Lithosphere of Central and Eastern Europe, Kyiv, Nauk. Dumka, 1988, P. 138-142 (in Russian)
11. Orlyuk M.I., Romenets A.A. Spatial-temporal change of the geomagnetic field: environmental aspect. Geoph. J., 2015, Vol. 42, No. 4, P. 18-38, DOI: https://doi.org/10.24028/gzh.0203-3100.v42i4.2020.210670_
12. M. Kanevski, M. Maignan, V. Timonin, A. Pozdnoukhov. Classification of interest rate curves using Self-Organising Maps. Presented at Applications of Physics in Financial Analysis conference (APFA6), Lisbon, Portugal, 2007, DOI: https://doi.org/10.48550/arXiv.0709.4401
13. Lucchini M., Bussi D. Self-Organizing Map. In: Maggino, F. (eds) Encyclopedia of Quality of Life and Well-Being Research. 2021, Springer, Cham. https://doi.org/10.1007/978-3-319-69909-7_104673-1

14. Ciampi A., Lechevallier Y. (2000). Clustering large, multi-level data sets: An approach based on Kohonen self-organizing maps. In Zighed D.A.; Komorowski J.; Zytkow J. (eds.). Principles of Data Mining and Knowledge Discovery: 4th European Conference, PKDD 2000 Lyon, France, September 13–16, 2000 Proceedings. Lecture notes in computer science. Vol. 1910. Springer, P. 353–358
15. Teuvo Kohonen. Self-Organizing Maps. Springer-Verlag, Berlin, Heidelberg, 2001. Series ISSN 0720-678X, 3 ver., DOI: https://doi.org/10.1007/978-3-642-56927-2
16. Vikas Kumar, Subhadip Ghosh, Manoj Kumar Parida, Shaju K. Albert. Application of continuous wavelet transform based on Fast Fourier transform for the quality analysis of arc welding process. Int. J. Syst. Assur. Eng. Manag. (2023). https://doi.org/10.1007/s13198-023-02178-7
17. W. Popinski, W. Kosek. The Fourier transform band pass filter and its application for polar motion analysis. Artificial Satellites, 1995, Vol. 30, No. 1, P. 9-25
18. Neubauer, G.P., Schimek, M.G. (1996). A Note on Cross-Validation for Smoothing Splines. In: Hardle, W., Schimek, M.G. (eds) Statistical Theory and Computational Aspects of Smoothing. Contributions to Statistics. Physica-Verlag HD. https://doi.org/10.1007/978-3-642-48425-4_13
19. Jacob T. VanderPlas. Understanding the Lomb-Scargle Periodogram. The Astrophysical Journal Supplement Series, 2018, Vol. 236, No. 1, P. 16
20. M.I. Ryabov, A.L. Sukharev, M.I. Orlyuk, L.I. Sobitnyak, A.A. Romenets. Comparative analysis of geomagnetic disturbance in the Odessa Magnetic Anomaly zone in the 24th cycle of solar activity. Radiophysics and Radioastronomy, 2019, Vol. 24, No. 1, pp. 68-79
21. Celso A.G. Santos, Bruno Soursa de Morais. Identification of precipitation zones within Sao Francisco River basin (Brazil) by global wavelet power spectra. Hydrological Sciences Journal, 2013, Vol. 58, No. 4, P. 789-796
22. G. Andre, M. Marcos, C. Daubord. Detection method of Meteotsunami events and characterization of harbour oscillations in Western Mediterranean. Conference June 2013: Coastal Dynamics 2013At: Arcachon, France. https://www.researchgate.net/publication/307974648_Detection_method_of_Meteotsunami_events_and_characterization_of_harbour_oscillations_in_Western_Mediterranean
23. F. Dandurand, T.R. Shultz. Automatic Maxima Detection: a Graphical User Interface and a Tutorial. Tutorials in Quantitative Methods for Psychology, 2011, Vol. 7, No. 2, P. 21-31
24. Kotsiaros S. Lithospheric Magnetic Anomalies from Satellite Data. In: Gupta, H.K. (eds) Encyclopedia of Solid Earth Geophysics. Encyclopedia of Earth Sciences Series, 2020, Springer, Cham. https://doi.org/10.1007/978-3-030-10475-7_276-1
25. Sukharev A.L., Orlyuk M.I., Ryabov M.I., Romenets A.A. On the first results of measurements of short-periodic variations of the geomagnetic field in the Odessa magnetic anomaly zone with second resolution. Radiophysics and Radioastronomy, 2018, Vol. 23, No. 2, P. 116-127
26. A. Sukharev, M. Orlyuk, M. Ryabov, L. Sobitniak, V. Bezrukovs, S. Panishko, A. Romenets. Results of comparison of fast variations of geomagnetic field and ionospheric scintillations of 3C 144 radio source in the area of Odessa geomagnetic anomaly. Astron. Astrophys. Trans., 2022, Vol. 33, Issue 1, P. 67–88